Ultraluminous X-ray Sources:
Supercritical Accretion onto Black Holes

L. Zampieri

INAF-Astronomical Observatory of Padova

ULTRALUMINOUS X-RAY SOURCES (ULXs)

They are the most powerful (persistent) point-like, off-nuclear X-ray sources in nearby galaxies, with $L >> L_{Edd}$ *for* $1\,M_\odot$ *(*$L > 10^{39}$ *erg/s).*

Several hundreds ULXs (or ULX candidates) are known nowadays (Liu & Bregman 2005, ROSAT catalogue; Swartz et al. 2004, Chandra archive; Walton et al. 2011, XMM-Newton catalogue).

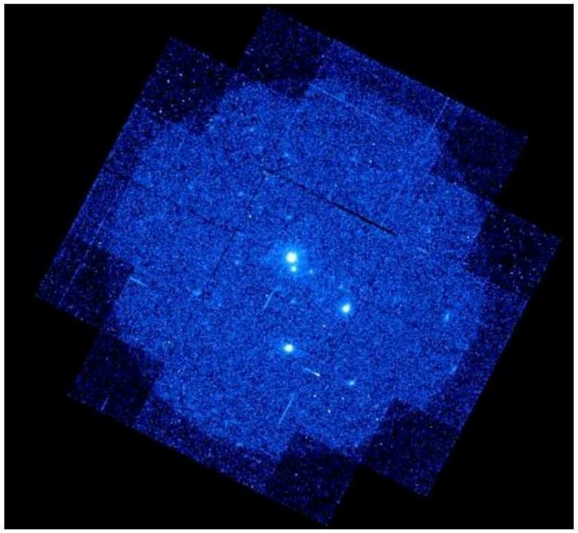

Figure 1: Three ULXs in the nearby spiral galaxy NGC 1313.

- $\sim 20\%$ Background AGNs
- $\sim 20\%$ Supernovae interacting with the circumstellar medium
- $\sim 60\%$ Accreting X-ray binaries (XRBs)

XRB nature (accreting black hole systems) supported by several observational evidences (e.g. Zampieri & Roberts 2009)

- High X-ray luminosity, X-ray spectra, short term variability
- Often in young stellar environments, stellar optical counterparts
- (Orbital) modulation in the X-ray and optical band, mass function of M 101 ULX-1 (Liu et al. 2013)
- Timing properties (QPOs)
- Correlation with host galaxy Star Formation Rate as for high mass XRBs, high luminosity end of the X-ray Luminosity Function of high mass XRBs

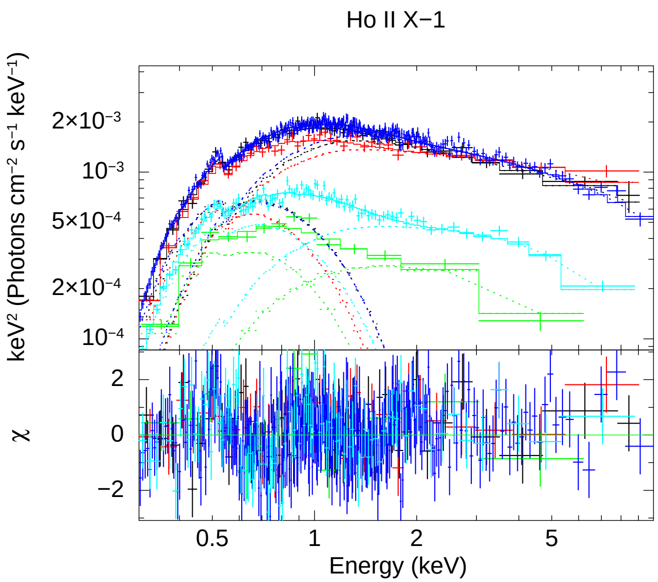

Figure 2: XMM spectra of Holmberg II X-1 (Pintore et al. 2014).

Many open questions on ULXs

But what type of XRBs are they? What is the origin of the exceptionally high isotropic luminosity?

What are the masses of the Black Holes (BHs) powering these sources?

What are the properties of their accretion flow?

What may ULXs tell us about stellar or intermediate mass BH formation?

And about extreme accretion environments?

Concerning the second question:

- Intermediate-mass BHs of $10^2 10^4\ M_\odot$ (Colbert & Mushotzky 1999)
- Stellar-mass BHs of $\sim 10\ M_\odot$ (King et al. 2001)
- Massive stellar BHs of $30 - 80\ M_\odot$ (Mapelli et al. 2009; Zampieri & Roberts 2009; Belczynski et al. 2010)

Concerning the third question:

- If intermediate-mass, ordinary sub-Eddington accretion: $L_{Edd} \approx 10^{41}$ erg/s for $M_{bh} = 10^3 M_\odot$
- If stellar-mass or massive BHs, a different (super-critical) accretion regime from Galactic BH binaries: $L_{Edd} \approx 10^{39} - 10^{40}$ erg/s for $M_{bh} = 10 - 80 M_\odot$

Apart from a handful of extremely luminous ($> 5 \times 10^{40}$ erg/s; Sutton et al. 2012) or hyperluminous ($> 10^{41}$ erg/s) objects, observationally BHs of several hundreds to thousands $M_\odot$ are not required for the majority of ULXs.

In the following we review the basics of accretion theory and focus on what is known about super-critical accretion onto stellar mass and massive BHs.

Accretion: Preliminaries

Motion of a test particle of mass m in the gravitational field of a compact object. Order of magnitude estimate of the energy that can be extracted:

$$\Delta E/mc^2 = GM_c/c^2 r_c = 0.15 (M_c/M_\odot)(r_c/10^6\,\mathrm{cm})^{-1} \quad \Longrightarrow \quad \text{compactness } M_c/r_c \tag{1}$$

Motion of a test particle in the Schwarzschild metric ($\epsilon = E/mc^2$, $h = L/m$, $\theta = \pi/2$):

$$\frac{\dot{r}^2}{c^2} + V_{eff} = \epsilon^2 \tag{2}$$

$$V_{eff} = \left(1 - \frac{r_S}{r}\right)\left(1 + \frac{h^2}{r^2 c^2}\right) \qquad r_S = 2GM/c^2 \tag{3}$$

$$V_{eff} = h^2/2r^2c^2 - GM/rc^2 \qquad \text{in the Newtonian case} \tag{4}$$

Maximum energy extraction: $\eta = V_{eff}(\infty)^{1/2} - V_{eff}(r_{ISCO})^{1/2} = 1 - \frac{2\sqrt{2}}{3} = 0.057$

where $r_{ISCO} = 3r_S$ is the innermost stable circular orbit (ISCO) and $h_{ISCO} = \sqrt{3}\, r_S \cdot c$.

In the Kerr metric: $\eta = 0.42$

Accretion luminosity ($\dot{M}$ accretion rate, mass accreted per unit time):

$$L_{acc} = \eta \dot{M} c^2 \simeq 10^{38} \eta_{0.1} \dot{M}_{-8}\,\mathrm{erg/s} \tag{5}$$

If this energy is transformed into thermal energy and then radiated without begin thermalized:

$$GMm_p/r_c \sim kT \qquad \Longrightarrow \qquad T \sim 10^{12}\,\mathrm{K} \sim 100\,\mathrm{MeV} \tag{6}$$

If radiation is thermalized (matter optically thick; LTE), the source emits as a blackbody:

$$L_{acc} = 4\pi r_c^2 \sigma T^4 \qquad \Longrightarrow \qquad T \sim 10^7\,\mathrm{K} \sim 1\,\mathrm{keV} \tag{7}$$

For a steadily radiating source and assuming spherical symmetry, the maximum luminosity above which accretion is quenched can be obtained setting the radiative ($F_{rad} = \sigma_T L/4\pi r^2$) force equal to the gravitational force ($F_g = GMm_p/r^2$) acting on a proton-electron pair:

$$L_{Edd} = 1.3 \times 10^{38} M_1\,\mathrm{erg/s} \qquad \text{Eddington luminosity for pure H} \tag{8}$$

$$\dot{M}_{Edd} = L_{Edd}/c^2 = 1.4 \times 10^{17} M_1\,\mathrm{g/s} \qquad \text{Eddington accretion rate} \tag{9}$$

Wind and Roche-lobe fed binary systems

WIND ACCRETION

Wind accretion is inefficient. Only owing to the high mass loss rates of early type stars, can X-ray binaries powered in this way be very luminous. However, too inefficient for persistent ULXs.

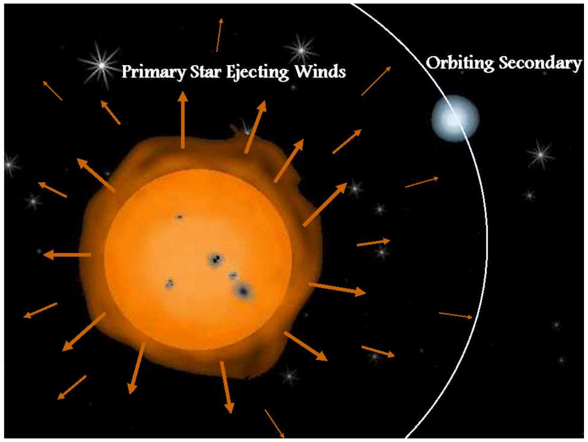

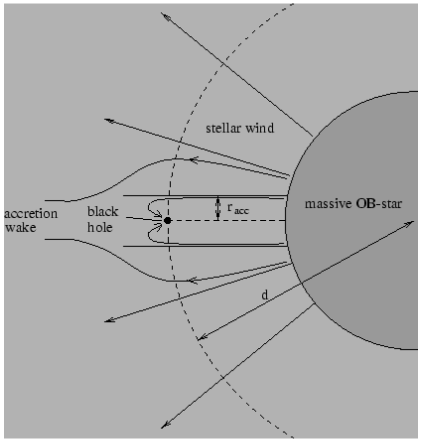

ROCHE-LOBE OVERFLOW

Motion of a test particle in the gravitational potential of two massive bodies (restricted three-body problem) in circular orbit about each other. In the reference frame corotating with the binary the motion is governed by the Roche potential:

$$\Phi_R = -\frac{GM_c}{|\mathbf{r} - \mathbf{r_c}|} - \frac{GM_*}{|\mathbf{r} - \mathbf{r}_*|} - \frac{1}{2}(\omega \times \mathbf{r})^2 \tag{10}$$

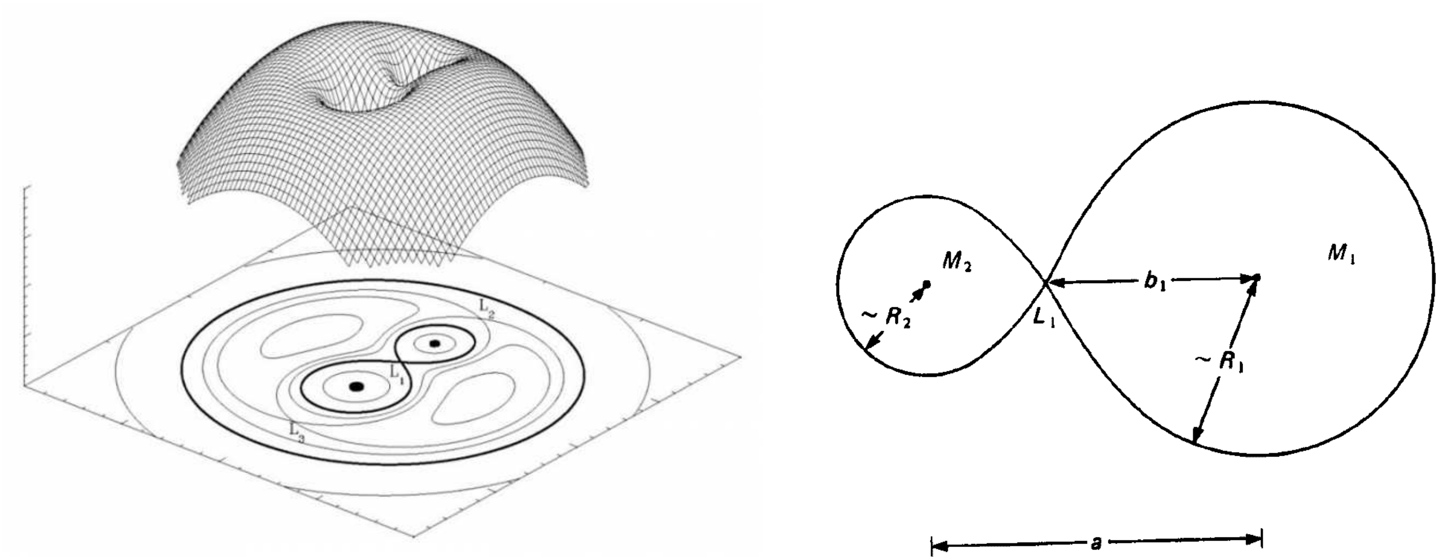

Figure 3: From Frank, King & Rayne (2002, Accretion Power in Astrophysics)

If at a certain stage of its evolution the companion star ($M_2 = M_*$) swells up so that its surface reaches contact with its Roche lobe R_2, any small perturbation will push material over the saddle point L_1 (inner Lagrange point) of Φ_R where it is eventually captured by the compact object.

If all mass lost by the secondary is accreted by the primary (conservative mass transfer):

$$\frac{(-\dot{M}_*)}{M_*} = \frac{1}{5/3 - 2q}\left(\frac{\dot{R}_2}{R_2} - 2\frac{\dot{J}_{tot}}{J_{tot}}\right) \tag{11}$$

where $q = M_*/M_c$. If $q < 5/6$ and the companion expands (e.g. when it becomes a giant/supergiant), $\dot{R}_2/R_2 > 0$ and the mass transfer is stable ($\dot{J}_{tot}/J_{tot} < 0$ because of gravitational radiation or magneto-hydro wind).

Specific angular momentum of the accreting matter:

$$l_R \sim R_1 \times (\omega_{orb} R_1) = 2\pi R_1^2/P \quad (12)$$

Radius R_0 where l_R is equal to the Keplerian angular momentum $l_K(R_0)$ (circularization radius):

$$R_0 \approx 1 P_{day}^{2/3} R_\odot >> r_c \qquad \Longrightarrow \qquad \text{formation of a ring} \quad (13)$$

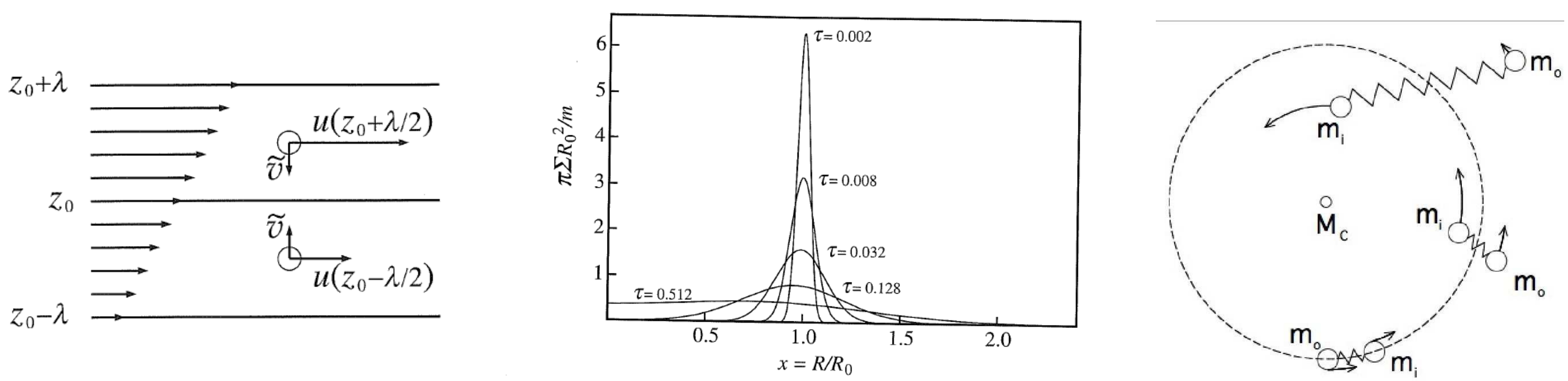

Figure 4: From Frank, King & Rayne (2002, Accretion Power in Astrophysics) and http://mri.pppl.gov/

If there is differential rotation, because of thermal or turbulent motion stresses are generated between neighbouring radii. The resulting effect is a net 'viscous' torque:

$$G = \nu \mu r^2 (\partial \Omega / \partial r) \tag{14}$$

As a consequence, the ring spreads out to form a disk.

Transition to turbulence in astrophysical accretion disks is via the magnetorotational instability (MRI; Balbus & Hawley 1991). The instability mechanism is essentially the coupling of the Keplerian shear flow, which represents a gradient in kinetic energy, by a magnetic field. A simple mechanical analogue for describing MRI is shown above.

Local structure of thin disks (standard SS model)

Basic Disk Equations

Hydrodynamic equations in cylindrical coordinates:

- mass conservation eq.
- radial momentum eq.
- angular momentum eq.
- energy conservation eq., including viscous heating and radiative heating/cooling

They are solved using standard assumptions:

- **Vertical integration**: $\int_0^h A(z)dz = hA(\eta) \approx hA(0/h)$
- $\Phi = \frac{GM}{(r^2+z^2)^{1/2}}$ Newtonian gravitational potential
- hydrostatic equilibrium in the vertical direction

$$\frac{1}{\rho}\frac{\partial P}{\partial z} - \frac{\partial \Phi}{\partial z} = \frac{1}{\rho}\frac{\partial P}{\partial z} + \frac{GMz}{(r^2+z^2)^{3/2}} = 0 \quad (15)$$

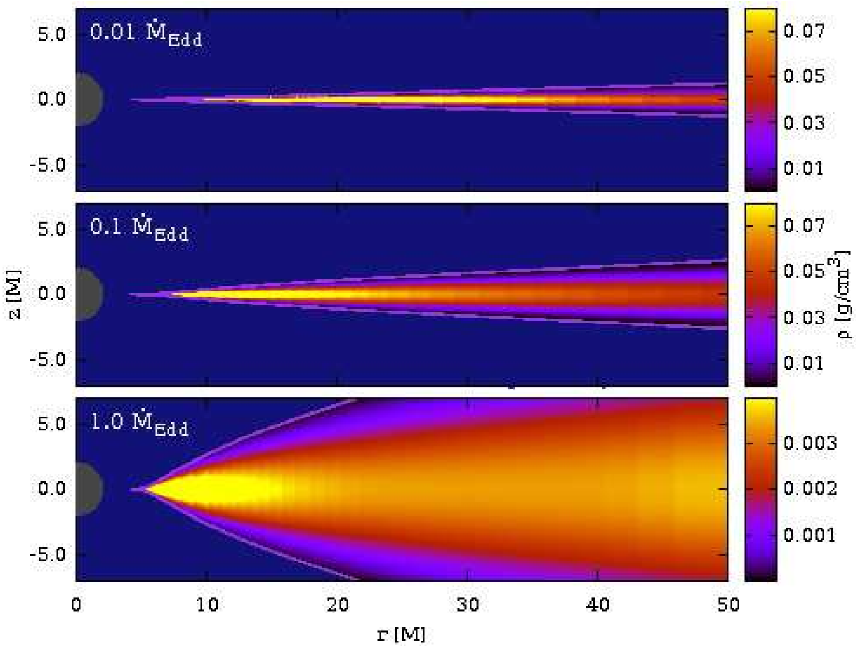

Local Structure of Newtonian Steady Thin Disks

- $v = -v_r \longrightarrow$ positive inward motion
- stationarity $\longrightarrow \partial/\partial t = 0$
- small radial velocity $\longrightarrow |v| \ll |v_\phi| = \Omega r$ (radial drift)
- disk geometrically **thin** $\longrightarrow h \ll r$
- *no energy advected* $\longrightarrow T\partial(v\mu s)/\partial r \ll G\Omega'$

$$4\pi v\mu = \dot{M} \tag{16}$$

$$\frac{v^2}{r} + (\Omega_K^2 - \Omega^2)r + \frac{v_s^2}{r} \approx 0 \implies \Omega \approx \Omega_K \tag{17}$$

$$\frac{\dot{M}}{4\pi} l = -\nu\mu r^2 \Omega' + C \implies \nu\mu = -\frac{\dot{M}}{4\pi r^2 \Omega'}(l - l_{in}) \tag{18}$$

$$rF(h) = \nu\mu r^2 (\Omega')^2 \implies 4\pi r F(h) = -\dot{M}\Omega'(l - l_{in}) \tag{19}$$

$$\frac{h}{r} \approx \frac{v_s}{v_K} \implies \text{local Kepler velocity highly supersonic}$$

$\mu = h\rho r$ linear mass density, Ω_K Keplerian ang. velocity, v_s sound velocity, F radiative flux

The electron plasma must be in thermal equilibrium and optically thick to photon emission-absorption ($\tau_{eff} = \sqrt{\tau_{abs}(\tau_{es} + \tau_{abs})} > 1$):

$$F(z) = -\frac{c}{3\kappa_R \rho} \frac{\partial a T^4}{\partial z} \tag{20}$$

κ_R is the Rosseland mean opacity. Integrating in the vertical direction:

$$F(h) \propto \frac{acT^4}{3\kappa_R \rho h} \tag{21}$$

Shakura-Sunyaev disks (standard or α disks; Shakura & Sunyaev 1973)

- Newtonian steady thin disks (Keplerian: $\Omega = \Omega_K$)
- α-viscosity prescription: $\nu = \alpha v_s h$
- Free-free or electron-scattering opacity:

$$\kappa_R = \kappa_{ff} = 3.7 \times 10^{22} (X+Y)(1+X) \rho T^{-3.5} g_{ff} \ \mathrm{cm}^2\ \mathrm{g}^{-1}$$

$$\kappa_R = \kappa_{es} = 0.2(1+X) \ \mathrm{cm}^2\ \mathrm{g}^{-1}$$

- Gas or radiation pressure dominated: $P = P_{gas} = \rho K T / \bar{\mu} m_p$ or $P = P_{rad} = a T^4/3$

With these assumptions the equations for Newtonian steady thin disks can be made explicit. Solution expressed in terms of 3 fundamental parameters: M, $\dot{M}$, α.

Different solutions according to the dominant pressure and opacity source

Outer free-free and gas pressure dom. region: $\kappa_{ff} > \kappa_{es}$, $P_{gas} > P_{rad}$

Intermediate electron-scattering and gas pressure dom. region: $\kappa_{ff} < \kappa_{es}$, $P_{gas} > P_{rad}$

Inner electron-scattering and radiation pressure dom. region: $\kappa_{ff} < \kappa_{es}$, $P_{gas} < P_{rad}$

Shakura-Sunyaev disk equations in the free-free and gas pressure dominated region

$$
\begin{aligned}
\Sigma &= 5.2\alpha^{-4/5}\dot{M}_{16}^{7/10} m_1^{1/4} R_{10}^{-3/4} f^{14/5}\ \mathrm{g\ cm^{-2}},\\
H &= 1.7\times 10^{8}\alpha^{-1/10}\dot{M}_{16}^{3/20} m_1^{-3/8} R_{10}^{9/8} f^{3/5}\ \mathrm{cm},\\
\rho &= 3.1\times 10^{-8}\alpha^{-7/10}\dot{M}_{16}^{11/20} m_1^{5/8} R_{10}^{-15/8} f^{11/5}\ \mathrm{g\ cm^{-3}},\\
T_c &= 1.4\times 10^{4}\alpha^{-1/5}\dot{M}_{16}^{3/10} m_1^{1/4} R_{10}^{-3/4} f^{6/5}\ \mathrm{K},\\
\tau &= 190\alpha^{-4/5}\dot{M}_{16}^{1/5} f^{4/5},\\
\nu &= 1.8\times 10^{14}\alpha^{4/5}\dot{M}_{16}^{3/10} m_1^{-1/4} R_{10}^{3/4} f^{6/5}\ \mathrm{cm^2\ s^{-1}},\\
v_R &= 2.7\times 10^{4}\alpha^{4/5}\dot{M}_{16}^{3/10} m_1^{-1/4} R_{10}^{-1/4} f^{-14/5}\ \mathrm{cm\ s^{-1}},\\
\text{with } f &= \left[1-\left(\frac{R_*}{R}\right)^{1/2}\right]^{1/4}.
\end{aligned}
$$

Figure 5: From Frank, King & Rayne (2002, Accretion Power in Astrophysics)

$\longrightarrow$ Relativistic standard thin disk equations derived by Novikov & Thorne (1973) and Page & Thorne (1974)

Shakura-Sunyaev disks

$\Longrightarrow$ $\Longrightarrow$ $\Longrightarrow$

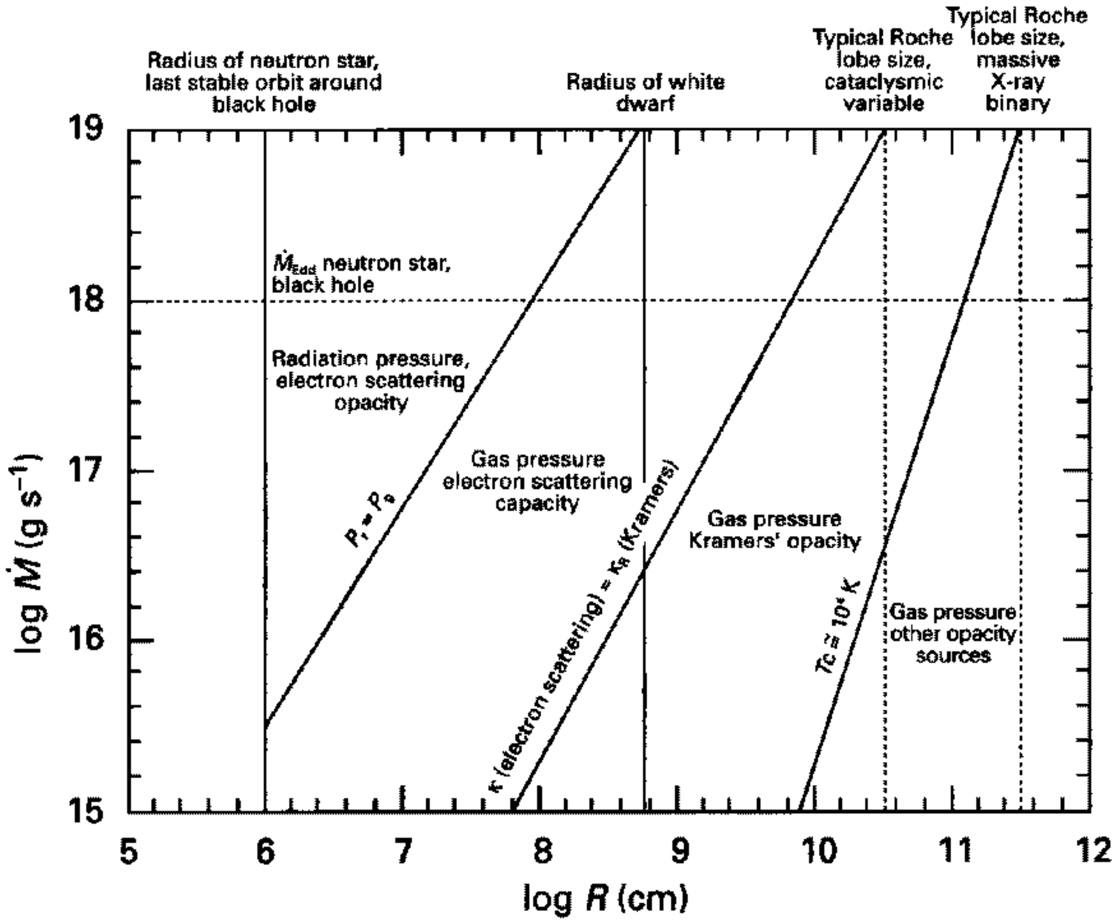

Figure 6: From Frank, King & Rayne (2002, Accretion Power in Astrophysics)

Disks with advection (slim disks) in ULXs with stellar-mass or massive BHs

If the assumptions that the disk is geometrically thin and no energy is advected are relaxed, the radial momentum and energy equations change:

$$v\frac{\partial v}{\partial r} + (\Omega_K^2 - \Omega^2)r + \frac{1}{\rho}\frac{\partial P}{\partial r} = 0 \tag{22}$$

$$4\pi r F(h) = -\dot{M}\Omega'(l - l_{in}) - B_1 \dot{M} T \frac{\partial s}{\partial r} \qquad F(h) = B_3 \frac{acT^4}{3\kappa_R \rho h} \tag{23}$$

Rotational velocity is no longer Keplerian and the temperature profile changes $\Longrightarrow$ Slim disk solutions (Abramowicz, Czerny, Lasota & Szuszkiewicz 1988; Watarai et al. 2000)

Advection of energy takes place because *radiative cooling becomes inefficient*:

- for $\dot{m} = \dot{M}/\dot{M}_{Edd} \ll 1$ the plasma becomes optically thin and density is too low (emissivity $\propto \rho^2$)
- for $\dot{m} > 1$ the density becomes sufficiently high that the photon diffusion timescale ($t_{diff} = \tau r/c$) is larger than the dynamical timescale ($t_{dyn} = r/v$): $\tau v/c > 1$.

Properties of slim disk solutions

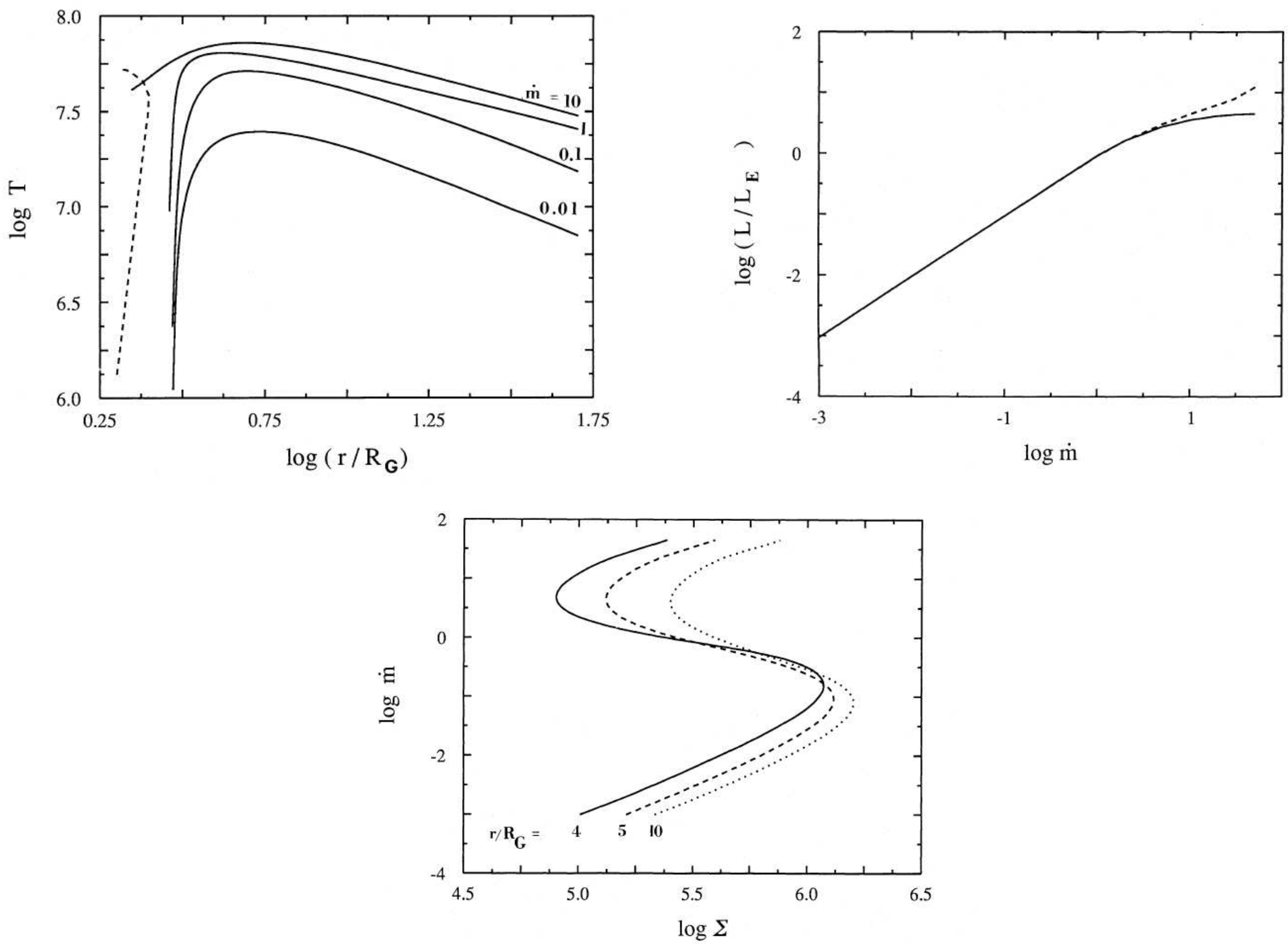

Figure 7: From Abramowicz et et al. (1988). $\Sigma = h\rho$ is the surface mass density. Because of energy advection, at very large $\dot{m}$ the luminosity $L \leq 5\, L_{Edd}$ (see also Watarai et al. 2000).

Disks with advection and outflows in ULXs with stellar-mass or massive BHs

Recent investigations of super-critical accretion have been carried out in 2 dimensional radiation-hydro simulations (e.g. Ohsuga et al. 2005, Ohsuga and Mineshige 2011). They show that the flow is composed of two parts: a disk region and an outflow region.

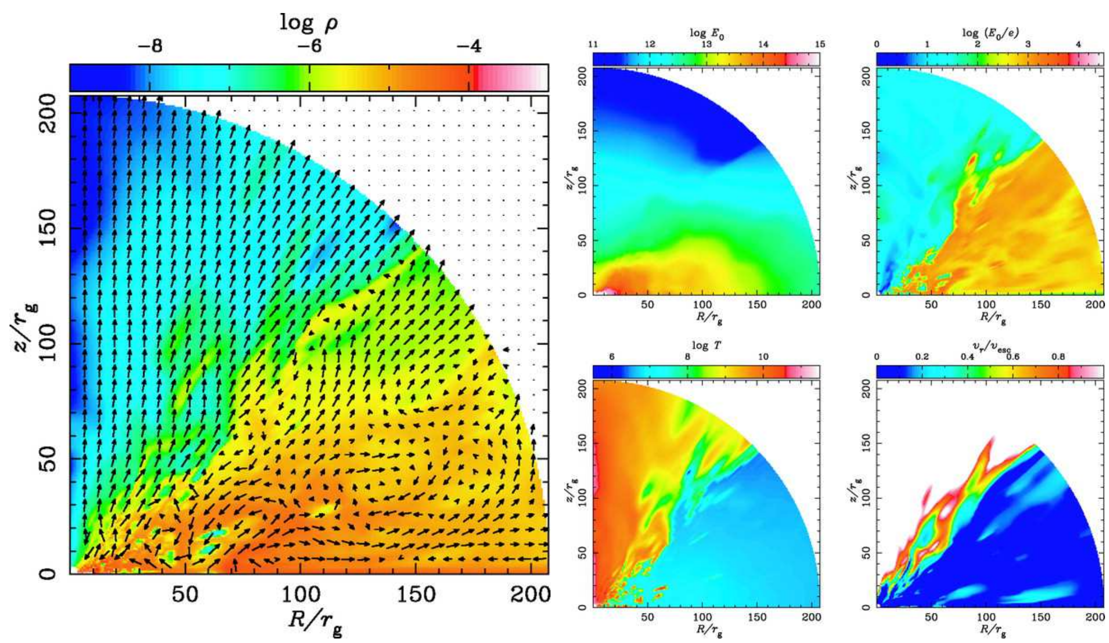

Figure 8: *Left*: Density distribution overlaid with the velocity vectors ($\dot{m}_{input} = 1000$). *Right*: Radiation energy density, ratio of the radiation energy to the (inertial) energy of the gas, gas temperature, and radial velocity normalized to the escape velocity.

Inside the disk circular motions and a patchy density structure is establisehd because of Kelvin-Helmholtz instability and (probably) convection. The mass accretion rate decreases inwards, while the remaining part of the disk material leaves the disk to form an outflow because of the strong radiation pressure force. Photon trapping is still important inside the disk.

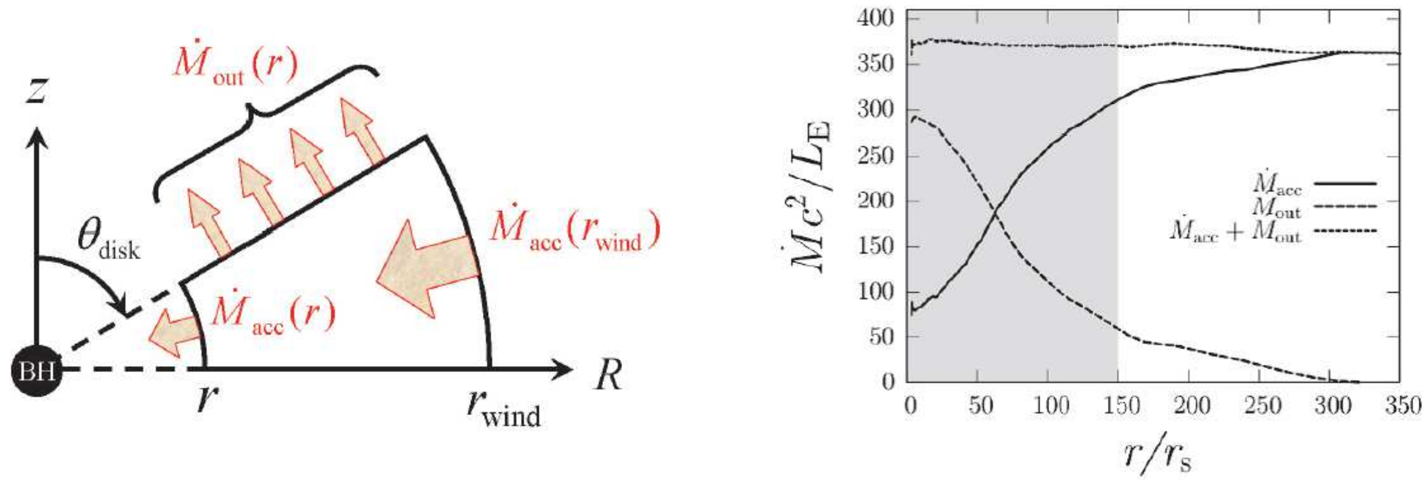

Figure 9: Below several Schwarzschild radii, the outflow is suppressed by photon trapping effects (Takeuchi et al. 2009)

.

Compared to the case without outflow, in the inner disk the density is greatly reduced, whereas the effective temperature distribution hardly changes $\Longrightarrow$ the emergent spectra do not sensitively depend on the mass outflow.

ULX SPECTRA AND SPECTRAL VARIABILITY

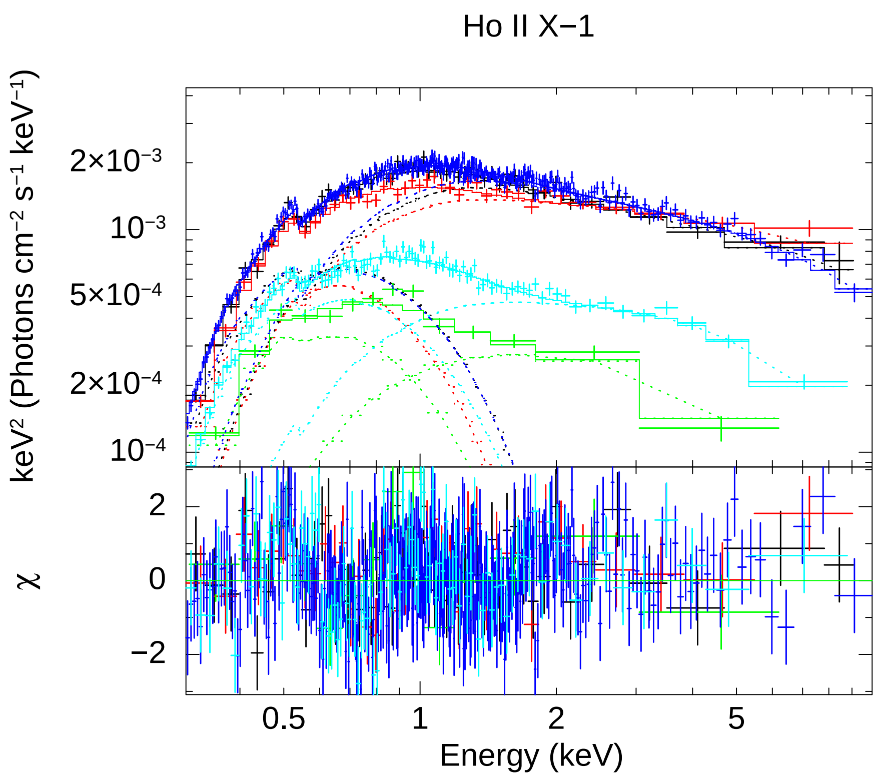

X-ray spectra and spectral variability can be explained in terms of the interplay between a supercritical (Comptonized) disk and a variable wind (Sutton et al. 2013; Pintore et al. 2014).